Functional Assembly of the Na^+/H^+ Antiporter of *Helicobacter pylori* from Partial Fragments in vivo†

Akira Karasawa, Keiji Mitsui, Masafumi Matsushita, and Hiroshi Kanazawa*

Department of Biological Sciences, Graduate School of Science, Osaka University, Machikaneyama-cho 1-1, Toyonaka City, Osaka, Japan

Received August 11, 2007; Revised Manuscript Received October 12, 2007

ABSTRACT: Functional assembly of the *Helicobacter pylori* Na^+/H^+ antiporter (HPNhaA) from partial fragments was studied. Expression plasmids encoding a series of complementary N- and C-terminal fragment pairs containing the transmembrane domains (TMs) were constructed by inserting a stop or a start codon into each of the loop regions of NhaA. HPNhaA fragments alone or complementary fragment pairs were expressed in Δ*nhaA Escherichia coli*, and fragment integration into the membrane and antiporter activity were measured. TM1−10, TM1−11, TM2−12, TM6−12, and TM10−12 were found in the membrane fraction, while the other fragments were not. While no single fragment displayed antiporter activity, simultaneous expression of fragments in certain pairs, such as TM1−2 + TM3−12, TM1−8 + TM9−12, or TM1−11 + TM12, reconstituted antiporter activity. With the exception of TM12, all of the fragments in the pairs were detected in the membrane. No single fragments expressed alone for these pairs were found in the membrane, except for TM1−11, suggesting that the interaction between the fragments in these pairs stabilized the fragments and enabled reconstitution of HPNhaA. We also found that the simultaneous expression of three complementary fragments (TM1−2 + TM3−8 + TM9−12) reconstituted HPNhaA activity. Other pairs that were found in the membrane (TM1−5 + TM6−12, TM1−10 + TM11−12, and TM1 + TM2−12) did not reconstitute antiporter activity, suggesting that they may not have the proper conformation. These results revealed that the ability to reconstitute antiporter activity depends on the split position in the loop regions and the interaction between complementary fragment pairs. We propose that formation of the active HPNhaA molecule is initiated by the interaction of short-lived intermediates and maintained by the increased stability of the intermediates within the resulting complex.

Na^+/H^+ antiporters are ubiquitous membrane proteins that occur in the plasma and organelle membranes of most organisms ranging from bacteria to humans (*1*−*5*). These antiporters are driven by the H^+ and Na^+ gradients across biological membranes in bacteria and mammalian cells, respectively. The antiporters play a major role in the pH and Na^+ homeostasis of cells (*1*−*5*). ECNhaA,[1] one of three Na^+/H^+ antiporters in *Escherichia coli*, plays a major role in the regulation of intracellular pH and cellular Na^+ concentrations in bacteria (*6*−*9*). NhaA has a highly conserved primary structure among many bacteria, including *Helicobacter pylori*, and is estimated to have 12 transmembrane domains (TMs) (*4*). The topology of TMs in NhaA has also been determined by *phoA* fusion analysis (*10*). Three Asp residues essential for ion transport, as well as several other functionally important residues, have been identified for ECNhaA (*11*) and *H. pylori* NhaA (HPNhaA) (*12*). These residues are clustered in TM4, -5, -10, and -11 in both HPNhaA (*12*) and ECNhaA (*11*).

An apparent pH-dependent antiporter activity has been characterized for ECNhaA, in which the antiporter activity is 2000-fold higher at pH 8.5 than that at pH 7.0 (*8*). In contrast, HPNhaA activity is consistently high across a broad pH range, from pH 6.5 to pH 8.5 (*13*). We have shown that the increase of HPNhaA activity at alkaline pH is associated with loop 7 and TM8, while the high activity at acidic pH is due to a structure formed by TM4 and TM10 (*12*). Recently, the structure−function relationships and topology of amino acid residues in HPNhaA TM4, -5, -10, and -11 were analyzed by cysteine scanning mutagenesis and *N*-ethylmaleimide probing of Cys residue accessibility (*14*, *15*, Y. Tsuboi, N. Kuwabara, and H. Kanazawa, unpublished results). These studies demonstrated that parts of TM4, -5, -10, and -11 face a water-filled channel-like structure. Asp141 and Thr140 in TM4 (*14*), Asp171 and Asp172 in TM5 (*15*), and Lys347 in TM10 (unpublished data) may constitute the binding site for transporting ions. Additionally, the crystal structure of ECNhaA has been determined at 3.45 Å resolution, indicating that these TMs form an ion transport

† The present study was supported by a Grant-in-Aid from the ministry of Education, Science, Sports, Technology and Culture of Japan.

* To whom correspondence should be addressed. E-mail: kanazawa@bio.sci.osaka-u.ac.jp. Phone: 06-6850-5812. Fax: 06-6850-5812.

[1] Abbreviations: NhaA, Na^+/H^+ antiporter A; GFP, green fluorescent protein; CFP, cyan fluorescent protein; Tricine, *N*-[2-hydroxy-1,1-bis-(hydroxymethyl)ethyl]glycine; TM, transmembrane domain; ACMA, 9-amino-6-chloro-2-methoxyacridine; FRET, fluorescence resonance energy transfer; SDS, sodium dodecyl sulfate; PAGE, polyacrylamide gel electrophoresis; HPNhaA, *Heliobacter pylori* Na^+/H^+ antiporter A; ECNhaA, *Escherichia coli* Na^+/H^+ antiporter A.

10.1021/bi701627e CCC: $37.00
Published on Web 11/16/2007

Table 1: Oligonucleotides Used for Constructing the Deletion Mutant of HPNhaA

oligonucleotide primer	sequence
pBR322-F	GATGCTGTAGGCATAGGC
pBR322-R	ACGATAGTCATGCCCCGC
HPTM1−2R	ATGTGCATGCCACTGGATAATTCCCCAAACA
HPTM1−4R	ATGTGCATGCCCTTGCCTAAAAGCATGATCA
HPTM1−6R	ATGTGCATGCCCATATTCAGGCGGTTTAATA
HPTM1−8R	TGTAAGGCGCTCGCTTTTTCCTCGCTTTTAATGAAGTTCT
HPTM1−10R	ATGTGCATGCCTGCGGTGATTTTAAGCTTTT
HPTM3−12F	GCAGGAATTCGAAAGAGAAATAAAAAATGTTCAAAAAAGCTTCTTTTCC
HPTM5−12F	GCAGGAATTCGAAAGAGAAATAAAAAATGAGGGTGCCAACCGCTTTAAA
HPTM7−12F	GCAGGAATTCGAAAGAGAAATAAAAAATGCGCTCGCTCATCCCTTACTT
HPTM9−12F	AGAACTTCATTAAAAGCGAGGAAAAAGCGAGCGCCTTACA
HPTM11−12F	GCAGGAATTCGAAAGAGAAATAAAAAATGCGCCCTAAAGGCATCAGCTG
HPTM1R	ATGTGCATGCCCCCAAAAGGGGTGTGCCATA
HPTM1−3R	ATGTGCATGCCAGCGTTAAGAAAAAAATAAA
HPTM1−5R	ATGTGCATGCCATTCGTGGTATAAAAGAGCG
HPTM1−7R	ATGTGCATGCCATGCACGCAAAACCAAAGCA
HPTM1−9R	ATGTGCATGCCGATGCTAGAATCAACGCTCA
HPTM1−11R	ATGTGCATGCCCTCGCTCGTGAAGGCCAGAT
HPTM2−12F	GCAGGAATTCGAAAGAGAAATAAAAAATGTTTCAAATAGGGGATTTTTT
HPTM4−12F	GCAGGAATTCGAAAGAGAAATAAAAAATGAACACGCCTTCCCAGCATGG
HPTM6−12F	GCAGGAATTCGAAAGAGAAATAAAAAATGTTAAAATTCGCATGGCTTTT
HPTM8−12F	GCAGGAATTCGAAAGAGAAATAAAAAATGCAAAGCGGTATCCATGCGAC
HPTM10−12F	GCAGGAATTCGAAAGAGAAATAAAAAATGAATTTAGAAGTGGATAAGGT
HPTM12F	GCAGGAATTCGAAAGAGAAATAAAAAATGCATAAAGACGCTATGGAAGT
ClaItetSDNhaAF	GCCCATCGATATGTTTGACAGCTTATCATC
ClaItetSDNhaAR	CGGGATCGATGTCGACTCATTTGTCGTCGT

pathway and part of the putative binding site for Na^+, Li^+, and H^+ (*16*).

The three-dimensional structure of ECNhaA (*16*) and precise biochemical analyses (*12*−*15*, *17*) have provided a detailed view of the structure−function relationships. However, questions have been raised as to how NhaA folds and is integrated into the membrane. Although NhaA is synthesized from the N-terminus to the C-terminus, the arrangement of the transmembrane domains is not necessarily ordered consecutively from the N-terminus, as indicated by the ECNhaA crystal structure (*16*). A hypothesis has recently been proposed for the biosynthesis of polytopic membrane proteins (*18*, *19*). According to this hypothesis, hydrophobic transmembrane domains are first inserted into the membrane as α-helices, and these helices next assemble to form the final native structure. This hypothesis is based on observations of transporters, including anion exchangers (*20*−*22*), and a G protein coupled receptor of yeast (*23*), by studying folding and assembly using partial polypeptide fragments. In these studies, partial fragments were independently and stably integrated into membranes and then reconstituted a functional transporter by association with other partial fragments. For the major facilitator superfamily (MFS) proteins containing 12 transmembrane domains, including lactose permease (LacY) (*24*) and the tetracycline transporter (TetA) (*25*), simultaneous expression of complementary N- and C-terminal halves of the molecules in vivo could reconstitute the active molecule. In these cases, stably expressed partial fragments were not detected, but rather, interactions between membrane domains in the two fragments were required to form an active molecule. Since the ECNhaA crystal structure revealed that the overall arrangement of transmembrane domains is different from that of other MFS proteins, it is not clear whether in vivo reconstitution of NhaA-like MFS proteins from complementary N- and C-terminal fragments is possible.

Here, to further our understanding of the in vivo processes involved in the formation of active NhaA, we examined whether partial fragments of HPNhaA can be stably expressed in the membrane as observed for G protein receptors (*23*) and anion exchangers (*20*). We surveyed a set of complementary N- and C-terminal fragments to determine whether they reconstituted an active NhaA upon simultaneous expression in *E. coli*. We found that certain combinations of complementary C- and N-terminal fragments reconstituted NhaA activity. These results suggested that in vivo formation of active NhaA depends on intramolecular interactions between the N- and C-terminal regions. This approach also enabled us to study the functional significance of the loop regions connecting transmembrane domains and revealed the functional importance of certain loops in integration of NhaA into the membrane.

MATERIALS AND METHODS

Bacteria Strains and Culture Conditions. E. coli strain HITΔ*AB*$^-$ (Δ*lacY*, Δ*nhaA*, *nhaB*$^-$) (*26*) was used for expression of HPNhaA fragments or HPNhaA fused to GFP variants, and JM109 (*27*) was used for construction of various other plasmids. Cells were cultured in L broth (LB) (*28*) containing 87 mM KCl instead of NaCl (LBK). For growth on solid plates, agar (1.5%, w/v) was added to the medium. Transformants were selected using the appropriate antibiotic. For analysis of salt resistance of HITΔ*AB*$^-$ transformed with various plasmids, additional amounts of NaCl or LiCl were added to LB plates (0.65 M NaCl, pH 7.5, or 0.15 M LiCl, pH 8.0). The plates and liquid cultures were incubated at 37 °C.

Construction of Plasmids Encoding HPNhaA Fragments. N-terminal fragments were amplified by PCR from the pBR-HP vector (*13*) using the pBR322-F primer and reverse primers (Table 1) which contained an *Sph*I restriction site

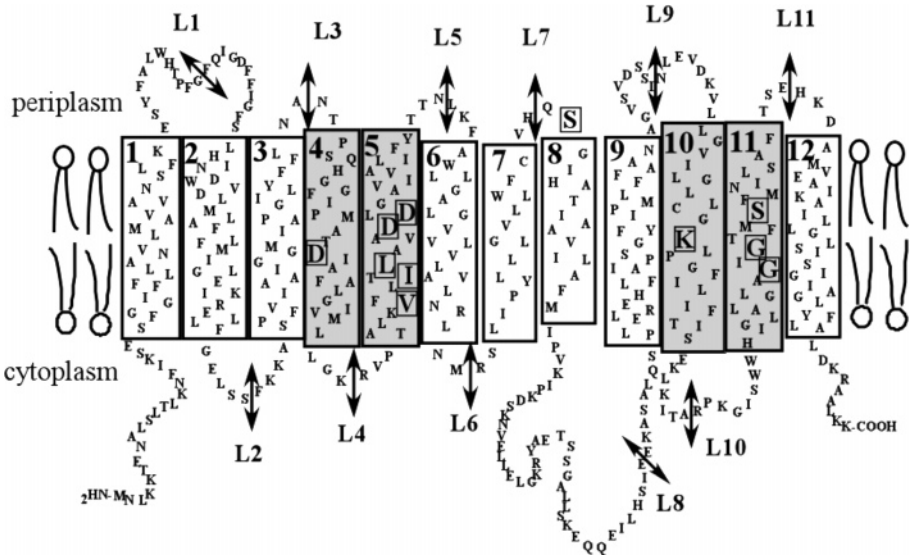

FIGURE 1: Secondary structure of NhaA of *Helicobacter pylori*. The *H. pylori* NhaA has 12 putative transmembrane domains. Essential and important residues (boxed) for ion transport activity are clustered in TM4, -5, -10, and -11, and these domains are thought to form the ion transport channel (*15*−*17*). Double arrows show the locations where fragment pairs were split in each loop.

(HPTM1−2R, HPTM1−4R, etc.). The PCR products were digested by *Eco*RI/*Sph*I and ligated to the *Eco*RI/*Sph*I fragment of pACYC-HP (*29*), creating pACYC−N-terminal fragment−FLAG vectors. C-terminal fragments were amplified by PCR from the pBR-HP vector using the pBR322-R primer and forward primers (Table 1) which contained an *Eco*RI restriction site, SD sequence, and start codon (HPTM3−12F, HPTM5−12F, etc.). The PCR products were digested by *Eco*RI/*Sph*I and ligated to the *Eco*RI/*Sph*I fragment of pBR-HP, creating the pBR−C-terminal fragment−FLAG vectors. For CFP fusions of the N-terminal fragments, the *Sph*I/*Sal*I fragment of CFP from an HPNhaA−CFP plasmid (*29*) was ligated to the *Sph*I/*Sal*I fragment of the pACYC−N-terminal fragment−FLAG vector. For the Venus fusions of the C-terminal fragments used in the FRET analysis, the *Sph*I/*Sal*I fragment of Venus from an HPNhaA−Venus plasmid (*29*) was ligated to the *Sph*I/*Sal*I fragment of the pBR−C-terminal fragment−FLAG vector. The plasmid encoding F_ob−Venus has been described previously (*29*). For simultaneous expression of three NhaA fragments, an expression vector encoding TM3−8 and TM9−12 fragments was constructed. The TM3−8 sequence was amplified by PCR from the pBR-HP vector (*13*) using the HPTM3−12F and HPTM1−8R primers shown in Table 1. The PCR products were digested by *Eco*RI/*Sph*I and ligated to the *Eco*RI/*Sph*I fragment of pBR-HP, creating the pBR−TM3−8 vector. Next, the TM3−8 sequence, including the *tet* promoter, SD sequence, and a *Cla*I restriction site, was amplified by PCR from the pBR−TM3−8 vector using the *Cla*I *tet*SDNhaAF and *Cla*I*tet*SDNhaAR primers shown in Table 1. The PCR products were digested by *Cla*I and ligated to the *Cla*I fragment of the pBR−TM9−12 vector (encoding the TM9−12 fragments), creating the pBR−TM3−8+TM9−12 vector.

Immunological Detection. Aliquots of membrane vesicles prepared from *E. coli* transformed with various NhaA fragments were subjected to SDS−PAGE, as described previously (*30*). The separated proteins were blotted onto GVHP filters (Millipore, Billerica, MA) and probed with anti-GFP (Molecular Probes, Inc.) or anti-FLAG (Sigma-Aldrich Corp.). Immunoreactive bands were visualized by enhanced chemiluminescence (Amersham Biosciences, Piscataway, NJ), as described previously (*30*). For whole cell fractions, *E. coli* (HITΔAB^-) transformed with plasmids encoding HPNhaA fragments were grown at 37 °C in LBK medium overnight and diluted to an OD_{600} of 1.0. Aliquots were subjected to SDS−PAGE and blotted, and the NhaA fragments were detected, as described above.

Preparation of Membrane Vesicles and Measurement of Na^+/H^+ Antiporter Activities. Membrane vesicles from *E. coli* cells transformed with various plasmids were prepared as described previously (*14*). After centrifugation of *E. coli* cells disrupted with a French press, the collected membrane vesicles (100 μg) were resuspended in 2 mL of assay buffer (10 mM Tricine and 140 mM KCl, adjusted to the desired pH with KOH), as described previously (*11*). Proton flow was measured by monitoring 9-amino-6-chloro-2-methoxyacridine (ACMA) fluorescence quenching after addition of potassium lactate (5 mM, pH 7.0) (*31*). Fluorescence dequenching, as a measure of the antiporter activity, was monitored with a fluorometer (JASCO FP-750, Jasco Ltd., Tokyo, Japan) after addition of 5 mM NaCl or LiCl.

FRET Analysis. All fluorescence measurements were performed using an FP-750 fluorometer (JASCO). FRET measurements using membrane vesicles from cells expressing fusion proteins were performed in Tricine−KOH buffer (10 mM Tricine, pH 8.5, 140 mM KCl). The membrane vesicles were irradiated at 433 nm to excite CFP, and fluorescence emission was recorded at 450−600 nm. Membranes were illuminated at 473 nm to excite Venus, and fluorescence emission was recorded at 500−600 nm. FRET was determined by subtracting the control emission spectra from the FRET emission spectrum. The control emission spectra were obtained by excitation of two types of control membranes, one expressing only CFP-tagged HPNhaA and the other expressing only Venus-tagged HPNhaA (*29*).

Gene Manipulation and DNA Sequencing. Preparation of plasmids, digestion of DNA with restriction endonucleases, ligation with T4 DNA ligase, and other techniques for handling DNA were performed according to published

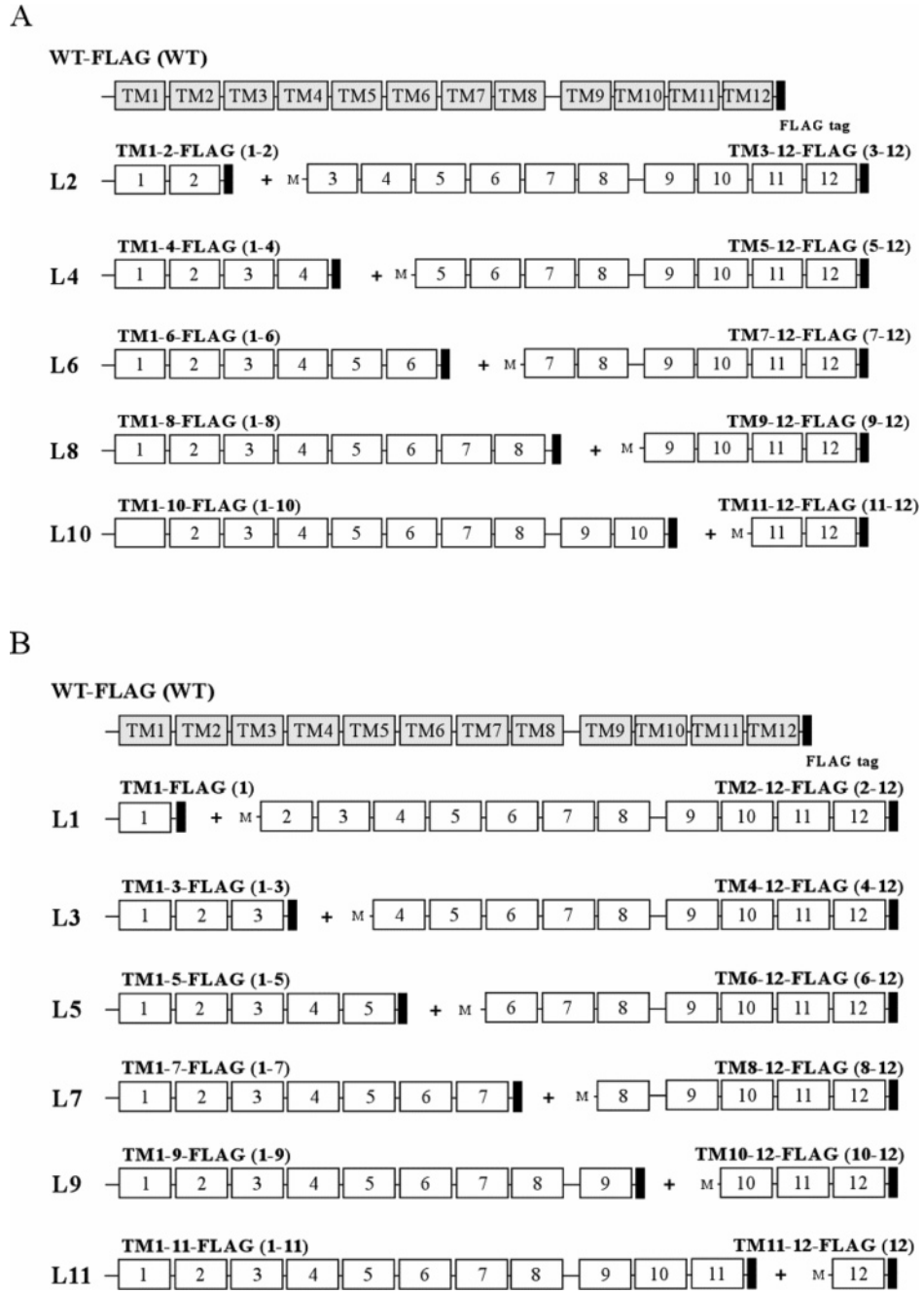

FIGURE 2: Schematic diagrams of the complemantary HPNhaA fragments constructed in this study. Various complementary fragments of HPNhaA split at each loop region are shown. The coding sequences of the N-terminal fragments were inserted into pACYC, while the C-terminal fragment sequences were inserted into pBR322 (Materials and Methods). These fragments were fused to a FLAG tag at the C-terminus. The C-terminal fragments contain an additional Met as an initiation codon. (A) NhaA fragments split at the cytoplasmic loop. B. NhaA fragments split at the periplasmic loop.

procedures (*32*). The nucleotide sequences of DNA fragments cloned into various expression plasmids in this study were verified using an automated sequencer (PE Biosystems, Foster City, CA).

Materials. Restriction endonucleases, T4 DNA ligase, Taq, and KOD DNA polymerases were purchased from Toyobo Co. (Osaka, Japan). Oligonucleotides were synthesized by Invitrogen (Carlsbad, CA); other reagents and materials were of the highest grade commercially available.

RESULTS

Construction of Expression Plasmids for HPNhaA Fragments. Expression of fragments containing complementary N- and C-terminal fragments of HPNhaA was studied to assess which NhaA fragments can be stably integrated into the membrane and, subsequently, which combinations of complementary fragments can reconstitute functional NhaA. For this purpose, expression plasmids encoding combinations of the complementary N- and C-terminal fragments were constructed by inserting a stop codon and an initiation codon into the loop region between two consecutive transmembrane domains (Figure 2). HPNhaA has 12 transmembrane domains, and each of these domains is connected by a hydrophilic loop (Figure 1). The hydrophilic loop sequences were based on the crystal structure of ECNhaA (*16*) and hydropathy plot analysis of HPNhaA (*30*). Eleven sets of

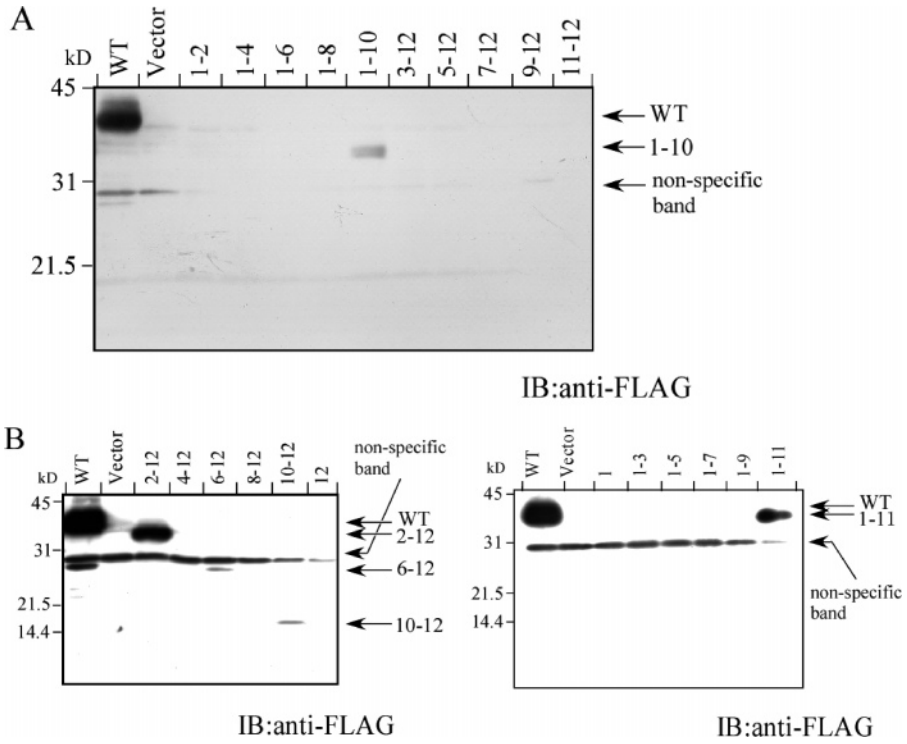

FIGURE 3: Detection of HPNhaA fragments expressed individually. Aliquots of membranes containing the different HPNhaA fragments were analyzed by Western blot using anti-FLAG antibodies (Sigma) and detected as described in the Materials and Methods. Abbreviations for the HPNhaA fragments correspond to those in Figure 2, and arrows at the right indicate the sizes of the fragments. Also, nonspecific bands are visible at around 30 kDa. (A) HPNhaA fragments split at a cytoplasmic loop. (B) HPNhaA fragments split at a periplasmic loop.

expression plasmids for complementary N- and C-terminal fragments were constructed (Figure 2). To express the complementary set in the same cell, the N- and C-terminal fragments were integrated into pACYC and pBR, respectively, which are expression plasmids with compatible replication origins. An additional Met residue was added at the N-terminus of each C-terminal fragment as the start codon, and then the FLAG tag sequence was added at the C-terminus of each fragments to detect expression by Western blotting.

Expression of N- and C-Terminal Fragments in the Membrane. We first examined whether individual fragments could be stably expressed in *E. coli* membranes. Each plasmid was introduced into HITΔAB^- cells and expression detected by Western blotting. The TM1−11 and TM 2−12 fragments were significantly expressed in spite of deletion of one TM, suggesting that the fragments were stable (Figure 3). TM1−10, TM6−12, and TM10−12 were weakly expressed, suggesting that these fragments of HPNhaA are integrated into the membrane in a relatively stable conformation. The other band detected around 30 kDa in all lanes is an endogenous *E. coli* protein that reacted with the anti-FLAG antibody, as it was also detected in the control lane containing proteins from the transformant with the vector alone. No other fragments were detected in the membrane fraction when expressed individually, even though these fragments contained significant hydrophobic TM domains and are found in the integral membrane regions of the *E. coli* crystal structure (*16*). Fragments not detected in the membrane fraction were also not found in the whole cell extract (data not shown). These results suggest that the fragments are not properly folded and are therefore not integrated into the membrane and/or are digested by proteases.

Abnormal membrane proteins are removed from the lipid bilayer and degraded by *E. coli* quality control mechanisms (*33*). This degradation may be prevented by fusion to a tightly packed hydrophilic protein such as GFP (*34*). Therefore, to clarify whether the undetected fragments were synthesized and then degraded, we fused the GFP variant CFP to the C-terminal fragments shown in Figure 4A. Expression of the CFP fusions in the membrane was detected by Western blotting using anti-GFP (Figure 4B). The previously undetected TM1−8 and TM1−2 were strongly and weakly detected, respectively, after CFP fusion, while the other fragments (TM1−4 and TM1−6) were not detected in the membrane even after fusion to CFP. Notably, TM1−8−CFP was detected, although TM1−8−FLAG was not found in the membrane. A GST fusion of TM1−8 was also detected (data not shown). These results suggest that TM1−8 was expressed but degraded and that fusion with a hydrophilic protein stabilized TM1−8 and/or protected it from protease attack. Next, we examined expression in the whole cell fraction by Western blotting with anti-GFP antibodies. Except for TM1−8−CFP, TM1−10−CFP, and WT−CFP, no bands corresponding to the other GFP fusions were detected. However, bands corresponding to the size of CFP were detected in cells expressing TM1−2−CFP, TM1−4−CFP, and TM1−6−CFP (data not shown). These results suggest that the TM1−2, TM1−4, and TM1−6 fragments are expressed but then degraded from the N-terminus.

Taken together, these results suggest that integration of the partial fragments into the membrane reflects the stable folding of the partial fragments and that stability depends on the region of NhaA included in the fragment, as well as the loop position where the fragment was cut. The stabilities of partial fragments of NhaA are classified into three

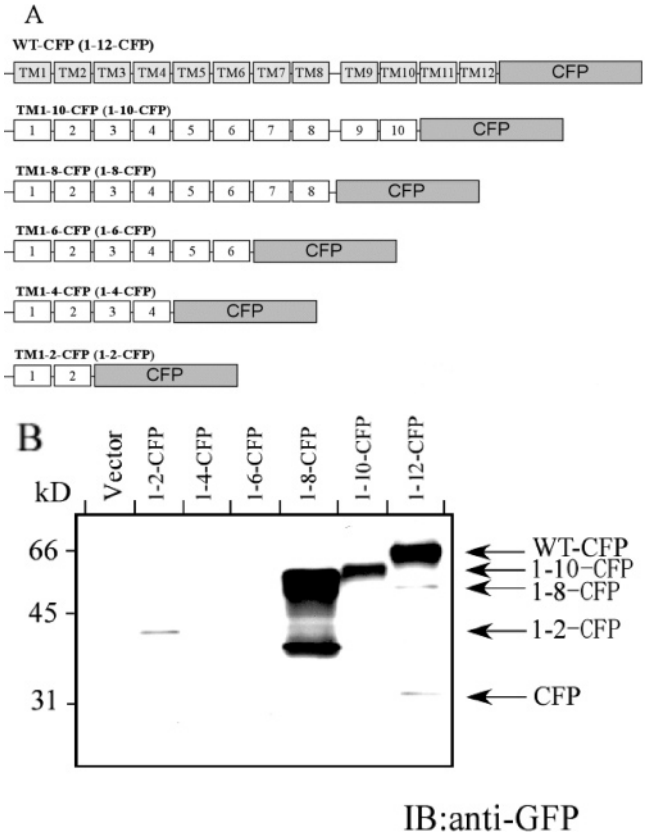

FIGURE 4: Schematic diagram and expression of CFP-fused HPNhaA fragments. (A) Schematic illustration of CFP fusions of HPNhaA fragments. CFP is fused at the C-terminus of each N-terminal fragment. (B) Aliquots of membranes containing the different CFP fusions of HPNhaA fragments were analyzed by Western blot using anti-GFP serum (Molecular Probe) and detected as described in the Materials and Methods. Abbreviations for HPNhaA fragments correspond to those in (A), and arrows at the right show the sizes of the CFP fusion fragments.

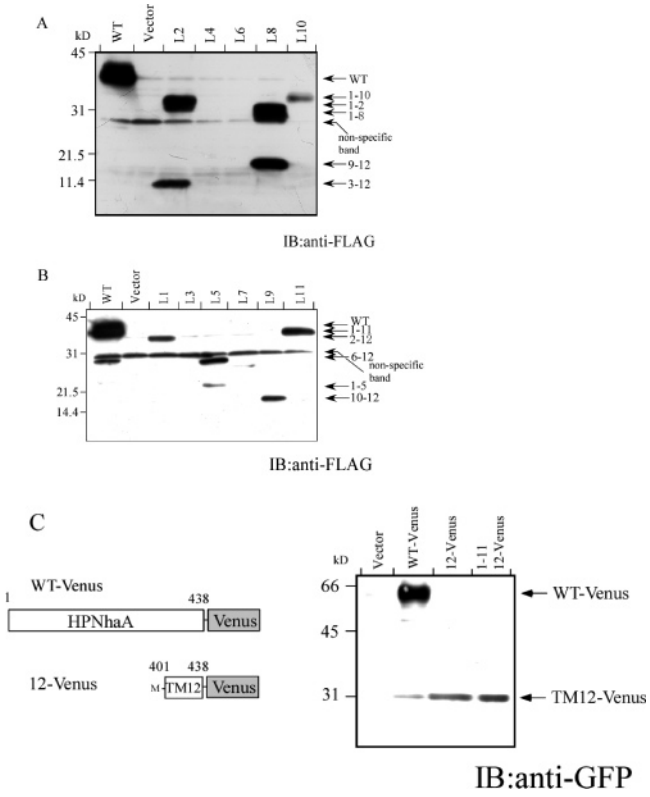

FIGURE 5: Coexpression of pairs of complementary fragments. Aliquots of membranes from cells coexpressing complementary fragments were analyzed by Western blot using anti-FLAG antibodies (Sigma) and detected as described in the Materials and Methods. Abbreviations for HPNhaA fragments correspond to Figure 2, and the arrows at the right show the sizes of the fragments. Also, nonspecific bands are visible at around 30 kDa. (A) HPNhaA fragments split at a cytoplasmic loop. (B) HPNhaA fragments split at a periplasmic loop. (C) Schematic diagrams of WT-HPNhaA−Venus and TM12−Venus are shown. Aliquots of membranes from cells coexpressing TM1−11−FLAG and TM12−Venus were analyzed by Western blot using anti-GFP serum (Molecular Probes) and detected as described in the Materials and Methods.

categories: (1) stable fragments, TM1−11, and TM2−12, (2) relatively stable fragments, TM1−10, TM6−12, and TM10−12, (3) conditionally stable fragments that were stabilized by the CFP fusion, such as TM1−8, and (4) unstable fragments, TM1, TM1−2, TM1−3, TM1−4, TM1−5, TM1−6, TM1−7, TM1−9, TM3−12, TM4−12, TM5−12, TM7−12, TM8−12, TM9−12, TM11−12, and TM12.

Coexpression of Pairs of Complementary HPNhaA Fragments. Next, various sets of complementary fragments of the N-terminal and C-terminal halves of HPNhaA split in a loop region (Figure 2) were tested for expression in the membranes. For TM1−2 and TM3−12 (L2 pair), TM1−5 and TM6−12 (L5 pair), and TM1−8 and TM9−12 (L8 pair), both fragments were detected (Figure 5A,B). Since none of the individual fragments in these combinations were detected in the membrane (Figure 3), these results indicate that simultaneous expression of the complementary fragments enables them to be integrated into the membrane as a stabilized form. For the complementary pairs TM1−10 and TM11−12 (L10), TM2−12 and TM1 (L1), and TM1−11 and TM12 (L11), the longer fragments were detected but the shorter fragments were not. In these cases, the longer fragments were detected when individually expressed (Figure 3). Therefore, expression of the longer fragments did not support expression of the complementary fragments (Figure 5). For the complementary pairs TM1−9 and TM10−12 (L9), TM10−12 was detected but the longer TM1−9 fragment was not. Although TM10−12 was detected when expressed alone (Figure 3), the presence of the complementary fragment further increased the amount of TM10−12 expressed (Figure 5). This result indicated that the simultaneous expression of TM1−9 and TM10−12 stabilizes only TM10−12. No expression was detected for the TM1−3 and TM4−12 (L3), TM1−4 and TM5−12 (L4), TM1−6 and TM7−12 (L6), and TM1−7 and TM8−12 (L7) fragment pairs.

Interaction between Complementary Fragments Detected by FRET. To demonstrate that the TM1−2 and TM3−12, or TM1−8 and TM9−12, fragments actually interact in the membranes, we conducted FRET experiments using the previously described methods (*29*). Plasmids encoding CFP or Venus fusions of the fragments were constructed, as shown in Figure 6A, and then the FRET signal between TM1−2−CFP and TM3−12−Venus, or TM1−8−CFP and TM9−12−Venus, in the membrane fraction was measured. As a negative control, FRET between the b subunit of the F_o ATPase−Venus (F_ob−Venus) and HPNhaA−CFP was measured. In Figure 6B, fluorescence spectra of membranes with NhaA−CFP alone are shown by the dotted lines. In membranes coexpressing TM1−2−CFP and TM3−12−

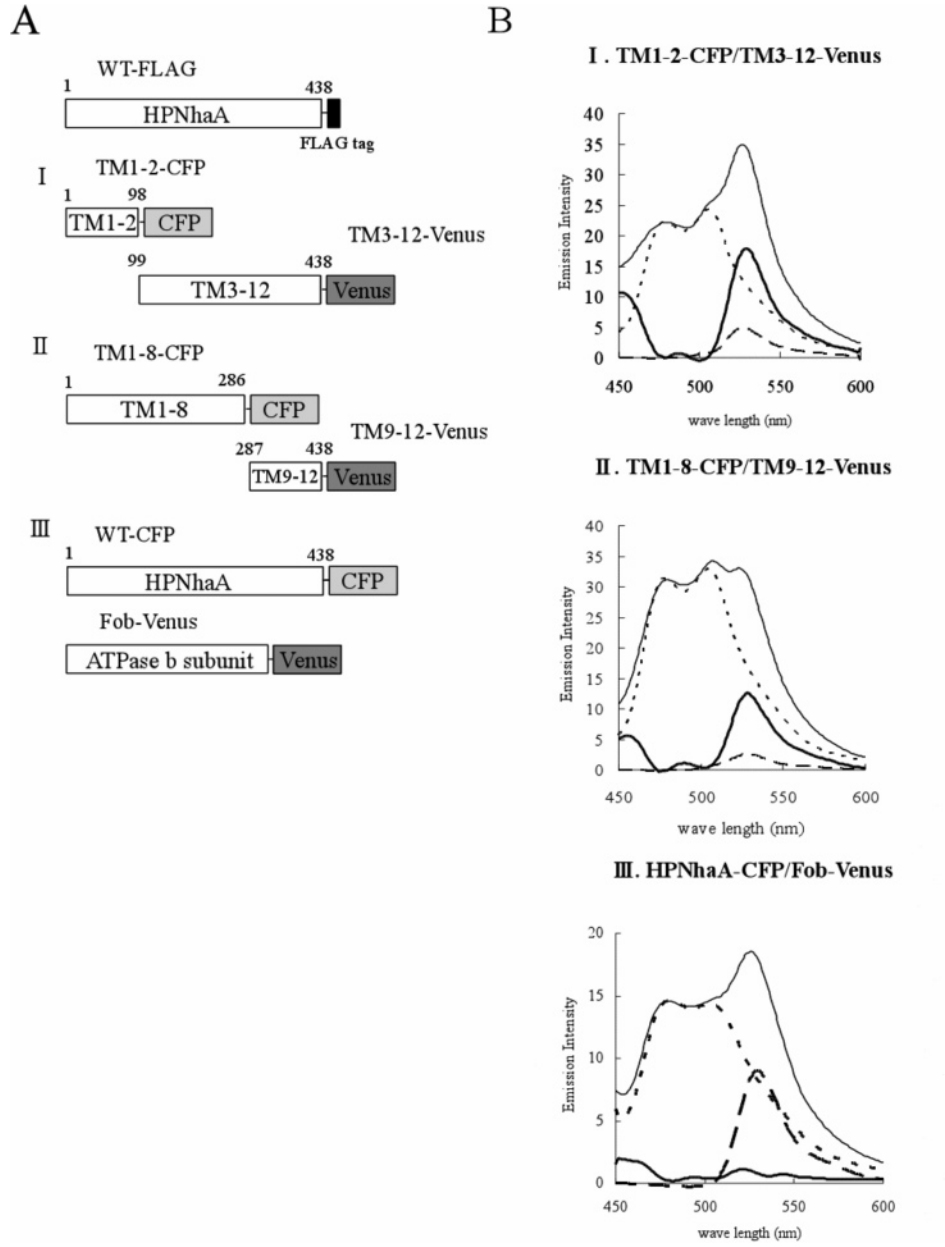

FIGURE 6: Schematic diagrams and fluorescence spectra of membranes containing GFP variant fusions of HPNhaA fragments. (A) Schematic illustration of CFP or Venus fusions of HPNhaA fragments and the F_o ATPase b subunit (F_ob). CFP and Venus were fused at the C-terminus of each fragment or of F_ob. (B) Fluorescence of membrane vesicles containing both CFP fusion and Venus fusion (thin line) was measured by exciting CFP with 433 nm light. Fluorescence of the membranes containing WT−CFP alone (dotted line) or WT−Venus alone (dashed line) in response to excitation at 433 nm was also measured. The FRET intensity (thick line) is shown by subtracting the fluorescence intensity spectra for WT−CFP alone (dotted line) and for WT−Venus alone (dashed line) from the fluorescence intensity obtained from membranes containing both CFP and Venus fusions (thin line).

Venus, the Venus fluorescence peak shifted to around 528 nm (maximum fluorescence for Venus) from 480 nm for CFP even when irradiated at the CFP excitation wavelength (Figure 6B, panel I). There was a slight direct excitation of Venus when membranes containing NhaA−Venus were illuminated with 433 nm light (dashed line). FRET can be calculated by subtracting the emission spectra of NhaA−CFP alone and NhaA−Venus alone from that of coexpressed NhaA−CFP and NhaA−Venus. The resulting FRET is shown by the thick solid line (Figure 6B). FRET was also detected between TM1−8−CFP and TM9−12−Venus (Figure 6B, panel II). These results demonstrate FRET between CFP and Venus, suggesting that the two fusion proteins are in close association. In contrast, when NhaA−CFP and F_ob−Venus were coexpressed, FRET was not detected (Figure 6B, panel III). This control experiment excludes the possibility that the FRET signal resulted from random collisions between NhaA fragments in the membrane.

Reconstitution of NhaA Antiporter Activity from Complementary Fragments. The presence of both complementary fragments in the membrane and their close association, as detected by FRET, suggested that the fragments reconstitute an active NhaA in vivo. To confirm this possibility, the growth of cells expressing the fragments on a high-salinity agar plate was tested and the NhaA activity was then measured using isolated membrane vesicles. While the Δ*nhaA* mutant cells could not grow at high salt concentrations, cells expressing certain sets of complementary frag-

Table 2: Growth of *E. coli* Cells Expressing the Complementary Fragments[a]

N-terminal half	C-terminal half	split position	cell growth Na^+	cell growth Li^+
wild type			++	++
without NhaA			−	−
TM1−2−FLAG	TM3−12−FLAG	loop 2	++	++
TM1−4−FLAG	TM5−12−FLAG	loop 4	−	−
TM1−6−FLAG	TM7−12−FLAG	loop 6	−	−
TM1−8−FLAG	TM9−12−FLAG	loop 8	++	++
TM1−10−FLAG	TM11−12−FLAG	loop 10	−	−
TM1−FLAG	TM2−12−FLAG	loop 1	−	−
TM1−3−FLAG	TM4−12−FLAG	loop 3	−	−
TM1−5−FLAG	TM6−12−FLAG	loop 5	−	−
TM1−7−FLAG	TM8−12−FLAG	loop 7	−	−
TM1−9−FLAG	TM10−12−FLAG	loop 9	−	−
TM1−11−FLAG	TM12−FLAG	loop 11	++	++
TM1−11−FLAG	TM2−12−FLAG	loop 1 or loop 11	+	+

[a] The complementary N- and C-terminal half fragments were expressed in *E. coli* HITΔAB^-. The cells were inoculated on LB plates with 0. 65 M (pH 8. 0) NaCl or 0.15 M (pH 7. 0) LiCl and incubated for 36 h. The cell growth yield on the plate was classified into three categories (−, +, ++) depending on the cell density on the plate.

ments (the L2, L8, and L11 pairs) could grow in high salt (Table 2). Cells with one fragment alone did not grow in high salt (data not shown). Na^+/H^+ antiporter activity was observed over the range of pH values tested for membrane vesicles of cells expressing L2, L8, or L11 pairs (Figure 7A,B). However, the Li^+/H^+ antiporter activity was low and in some cases less than the basal level in the alkaline pH range, while the activity was high in the acidic pH range (Figure 7B). These results confirmed that the combinations of TM1−2 and TM3−12 (L2 pair) or TM1−8 and TM9−12 (L8 pair) reconstituted an active NhaA structure, although the structures are not identical to the wild-type NhaA. The complementary CFP or Venus fusion fragments used for FRET analysis also showed antiporter activity (Figure 7). The L11 pair (TM1−11 and TM12) possessed approximately 60% of the wild-type activity (Figure 7C,D). The TM12 fragment was not found in the membrane, and the TM1−11 fragment did not have activity when expressed alone (Figure 5B and Table 2). These results suggest that TM1−11 is sufficient for NhaA activity, but only when expressed with TM12. This hypothesis, in turn, suggests that TM12 must be present in the membrane. Indeed, when the TM12−Venus fusion was coexpressed with TM1−11, both TM12−Venus and TM1−11 were detected (Figure 5C) and the antiporter activity was similar to that for TM1−11 and TM12 (Figure 7D). This result raises the possibility that TM12 may not be detected, even though it was present in the membranes when expressed alone. The L5 pair did not show antiporter activity, although TM1−5 and TM6−12 were detected in the membranes (Table 2 and Figure 5B). Other fragments that were found in the membrane when expressed alone did not show antiporter activity when expressed with their complementary fragment.

Reconstitution of NhaA Activity from three Fragments. The reconstituted NhaA activity of the L2, L8, and L11 pairs suggested that cleavage at these positions might allow stable integration of the fragments into the membrane. The results also raised the possibility that TM1−2, TM3−8, and TM9−12 might be able to reconstitute an active NhaA antiporter if they were expressed together. As shown in Figure 8A, high NhaA antiporter activity was observed when the three fragments were expressed together, and all three fragments were detected in the membrane (Figure 8C). However, their pH-dependent Li^+/H^+ antiporter activity was different from that of the wild type (Figure 8B) and resembled that of the Li^+/H^+ antiporter reconstituted from L2 and L8 pairs (Figure 7B). The pH-dependent profile of the antiporter activity of reconstituted NhaA was not exactly the same as that of the wild type, although it had significant Na^+/H^+ antiporter activity. Protein bands corresponding to TM1−2, TM3−8, and TM9−12 were observed on SDS−polyacrylamide gels (Figure 8C). Although TM3−8 and TM9−12 were detected at a high level, the amount of TM1−2 was lower than that of the two other fragments. Since TM1−2 is small, it may be degraded or pass through the membrane filter during Western blotting. Besides the three major bands, two weak bands (A and B in Figure 8C) were also observed. These might correspond to aggregates of the three fragments.

DISCUSSION

In this study, stable integration of partial HPNhaA fragments into the membrane and reconstitution of NhaA activity from the fragments were studied. Additionally, the loop structures connecting consecutive transmembrane domains that are important for integration of a fragment into the membrane were determined. We found that three complementary N- and C-terminal pairs of the fragments, TM1−2 + TM3−12 (L2 pair), TM1−8 + TM9−12 (L8 pair), and TM1−11 + TM12 (L11 pair), could reconstitute Na^+/H^+ antiporter activity in vivo. Both fragments in these pairs were detected in the membrane when coexpressed, with the exception of TM12. However, only TM1−11 was detected when these six fragments were expressed individually. Since no individual fragments, including TM1−11 (Figure 2), displayed antiporter activity, the presence of both complementary pairs must be required to reconstitute the activity. For the L2 and L8 pairs, during integration of the fragment into the membrane, interactions among the complementary pairs probably stabilize the fragments and lead to formation of an active NhaA molecule. In fact, interaction of the complementary fragments of the L8 and L2 pairs was confirmed by FRET analysis. The expressed levels of the fragments in the two pairs are not necessarily stoichiometric. The smaller fragments, TM1−2 and TM9−12, are less than the larger fragments, TM3−12 and TM1−8. The smaller fragments might be degraded in cells or lost during blotting from a polyacrylamide gel to a membrane filter more than the larger ones. When TM1−11 was coexpressed with TM12−Venus, TM12−Venus as well as TM1−11 was detected in the membrane fraction and the antiporter activity was similar to that of TM1−11 + TM12. These results suggested that TM12 is present in the active complex even though it was not detected by Western blotting.

We asked why only the L2, L8, and L11 pairs, but not other fragment pairs, were able to reconstitute the antiporter activity. One factor may be the position at which the NhaA is split into two fragments. For example, the loop position where the protein was split in the L2, L8, and L11 fragment pairs may not affect the correct integration of the two TMs flanking the loop, while splits at other loops may prevent the flanking TMs from properly integrating into the mem-

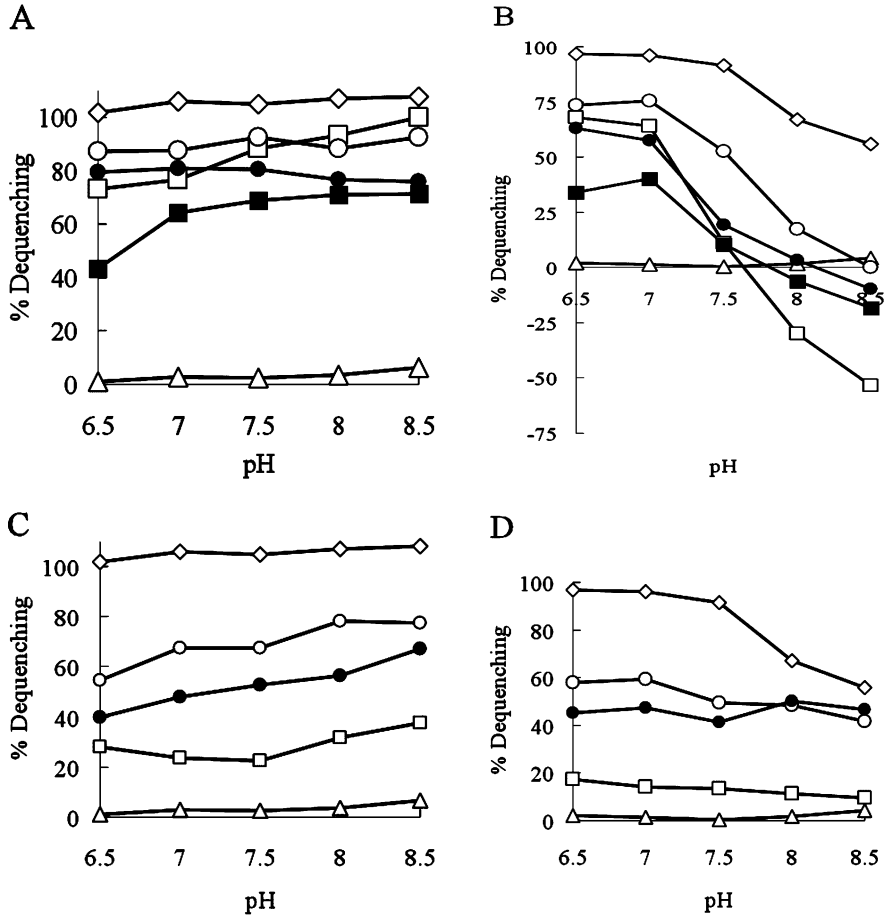

FIGURE 7: Antiporter activity of HPNhaA reconstituted from complementary fragments. pH-dependent Na^+/H^+ antiporter activities in membranes containing various complementary fragments are shown in (A) and (C). pH-dependent Li^+/H^+ antiporter activities in membranes containing various complementary fragments are shown in (B) and (D). Membrane vesicles were prepared from *E. coli* (HITΔAB^-) containing the complementary fragments. Membrane vesicles (100 μg) were incubated in 2 mL of assay buffer, and the pH-dependent antiporter activity was measured as the change in ACMA fluorescence driven by 5 mM lactate and 5 mM NaCl (A, C) or 5 mM LiCl (B, D). The percentage of fluorescence dequenching observed before and after addition of NaCl or LiCl is plotted against the assay pH. Key: WT, open tilted squares; vector, open triangles; L8 pair (Figure 2), open circles in (A) and (B); L2 pair, open squares in (A) and (B); TM1−2−CFP/TM3−12−Venus, closed squares; TM1−8−CFP/TM9−12−Venus, closed circles; L11 pair, open circles in (C) and (D), TM1−11−FLAG/TM2−12−FLAG, open squares in (C) and (D); TM1−11−FLAG/TM12−Venus, closed circles in (C) and (D).

brane. Significant interactions between some adjacent TMs in the final structure and/or during maturation of the NhaA molecule may be required. Unstable fragments may not be integrated into the membrane or may be inserted, but later degraded by proteases, including FtsH (*33*).

Since the L8 loop is the longest loop (50 residues) (Figure 1), interactions between TM8 and TM9 may not be required for integration into the membrane. This hypothesis is supported by the observation that TM8 and TM9 are separated by TM2 and no TM8−TM9 interaction is observed in the ECNhaA crystal structure (Figure 9). Since the hydrophilic regions in the loops in which the L2 and L11 pairs were split are shorter than the L8 loop, interactions between the two consecutive transmembrane domains may be more likely than between TM8 and TM9. However, TM2 and TM3 are separated by TM4 and TM5 and located in different regions within the ECNhaA crystal structure (Figure 9). These observations suggest that splitting the protein between these TMs allows a suitable conformation for reconstitution of antiporter activity. To further test whether the location of the split determines stable integration into the membrane, we tested whether simultaneous expression of three fragments, TM1−2, TM3−8, and TM9−12, could reconstitute an active NhaA antiporter, since the locations of these splits should not affect integration of the fragments into the membrane. As shown in Figure 8, activity was reconstituted under these conditions, which is in support of this hypothesis. As shown in Figure 3, TM1−11 is stably expressed without TM12, suggesting that the location of the split in the L11 pair does not affect integration of TM1−11 and, possibly, TM12.

For the L5 pair, interactions between TM5 and TM6 are not significant in the crystal structure, consistent with the stable expression of TM1−5 and TM6−12. However, antiporter activity was not reconstituted. These observations strongly indicate that continuity between these regions is essential for proper folding of the NhaA. The other fragment pairs which did not reconstitute activity, L1, L3, L4, L6, L7, L9, and L10, may also require an intact loop between the TMs where the protein was split for proper integration into the membrane. For TM3 and TM4 (L3), TM4 and TM5 (L4), TM6 and TM7 (L6), TM7 and TM8 (L7), and TM10 and TM11 (L10), the consecutive TMs are closely associated in the crystal structure (Figure 9). Additionally, the relative hydrophobicity of two consecutive TMs may affect mutual integration of the domains into the membrane. It has been

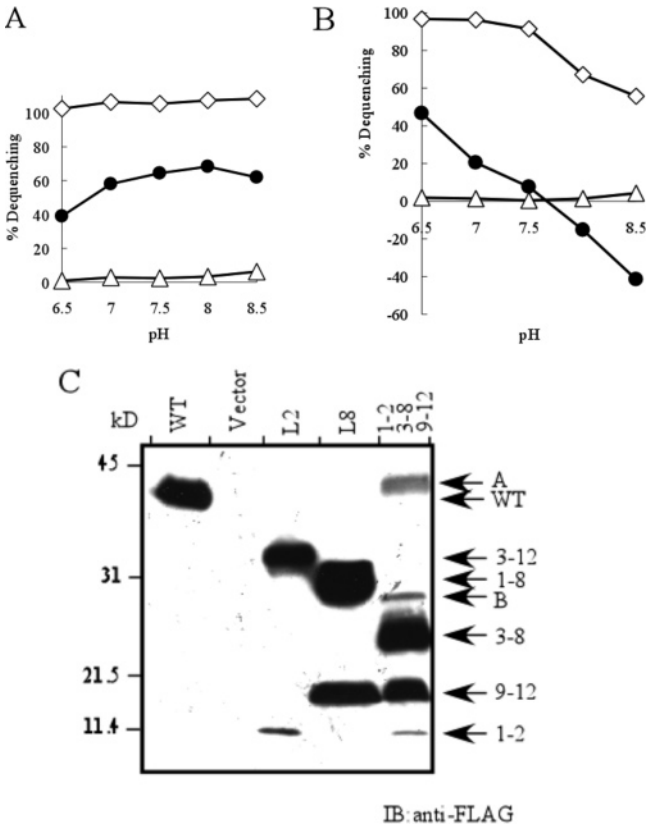

FIGURE 8: Reconstitution of NhaA activity from three split fragments. Reconstitution of the antiporter activity of HPNhaA from three complementary fragments. Membrane vesicles coexpressing TM1−2, TM3−8, and TM9−12 were prepared from HITΔ*AB*$^-$, and pH-dependent Na^+/H^+ (A) or Li^+/H^+ (B) antiporter activities were measured. (C) The three split fragments were analyzed by Western blot using anti-FLAG antibodies (Sigma) and were detected as described in the Materials and Methods. To assign the positions of the three split fragments, the complementary fragments in the L2 and L8 pairs were also subjected to electrophoresis. Abbreviations for the HPNhaA fragments correspond to those in Figure 2. "3−8" indicates TM3−8. Arrows at the right indicate the sizes of the fragments.

reported that if one TM is relatively hydrophilic and the other hydrophobic, the hydrophobic domain pulls the relatively hydrophilic domain into the membrane (*35*). Thus, a split in the loop connecting two such TMs would affect normal integration of the TMs into the membrane. These observations support our current hypothesis that some loops may play a role in integration of TMs into the membrane. In cases where the TMs do not interact in the ECNhaA crystal structure, as with the L1 and L9 fragments pairs, for example (Figure 9), the mechanism by which the split affects integration of the fragments into the membrane remains to be determined. For the complementary fragment pairs in which the N-terminus of the C-terminal fragment faces the periplasm (L1, L3, L5, L7, L9, and L11), the N-terminus may not be able to integrate into the membrane. Since among these pairs only L11 could reconstitute an active NhaA antiporter, our prediction may be correct. However, further systematic analyses of the integration of these C-terminal fragments into the membrane may be required, including an analysis of the integration of TM2−12, which was stable in the membrane but ineffective for the reconstitution of antiporter activity when expressed with TM1. Finally, the location of the split may cause improper folding of the fragments, which would lead to degradation by proteases such as FtsH (*33*).

When individual fragments were expressed, TM1−11 and TM2−12 alone were detected. The expression of TM1−10 and TM3−12, in which TM11 and TM2 are missing, respectively, was very low. The expression of other fragments was also null or very low (TM6−12 and TM10−12). These results suggested that TM11 and TM2 may play a key role in stabilizing the fragments. In the crystal structure (Figure 9), these TMs are located in the center of the structure and interact with many other TMs. In contrast, TM12 and TM1 are located at the most outer region of the crystal structure and interact with only a few TMs. Thus, it seems possible that interactions between TMs may also contribute to the stability of the partial fragments. If TM2 is lost, residues such as hydrophilic residues in the TM8 or TM9 closely located to the seven hydrophilic residues in TM2 (Figure 9) (*16*) might be exposed to a hydrophobic environment. This would lead to instability of TM3−12 without TM2.

TM1−8 was not detected when expressed alone, indicating that the fragment is unstable. However, fusion of a GFP variant at the C-terminus of TM1−8 stabilized the fragment, suggesting that the relatively long C-terminal hydrophilic tail of TM1−8 is susceptible to attack by a protease such as FtsH. This observation is consistent with previous data indicating that FtsH attacks a relatively long hydrophilic region of membrane proteins (*33*). Stable expression of TM1−8 and the GFP variant fusion suggested that TM1−8 was integrated into the membrane before degradation. The attachment of the GFP variant to the C-terminal end of a fragment protected the transmembrane fragment from proteolysis. This suggests that the attachment of the GFP variant to membrane proteins might provide a useful method to improve the expression of unstable membrane proteins or transmembrane helices in general.

For several polytopic membrane proteins, including CLC-1 (*36*), CFTR (*37*), GPCR (*23*), bacteriorhodopsin (*38*, *39*), rhodopsin (*40*, *41*), AE1 (*20*−*22*), LacY (*24*, *42*), TetA (*25*), NaPi-2 (*43*), and Sec61p (*44*), some combinations of complementary fragments can reconstitute the active complex or native conformation. For CLC-1, CFTR, GPCR, bacteriorhodopsin, AE1, NaPi-2, and Sec61p, partial fragments alone could be stably expressed in the membrane, suggesting that each fragment contains sufficient information to be integrated into the membrane and folds independently. A two-stage model was proposed for the biogenesis of membrane proteins such as these. This model postulated that transmembrane domains fold independently after integration into the membrane and then later associate to form a final structure without significant rearrangement of their original conformation. In contrast, for rhodopsin (*45*), LacY (*24*), and TetA (*25*) some of the partial fragments are expressed as semistable intermediates but were stabilized by simultaneous expression of the N- or C-terminal complementary partner. These results are similar to our present findings with HPNhaA: semistable partial fragments of NhaA interact and become stable in the active final structure. The stable intermediate state proposed by the former hypothesis may not exist for NhaA. These results suggest that, for a polytopic membrane protein, formation of an active molecule is initiated by short-lived intermediates which readily interact

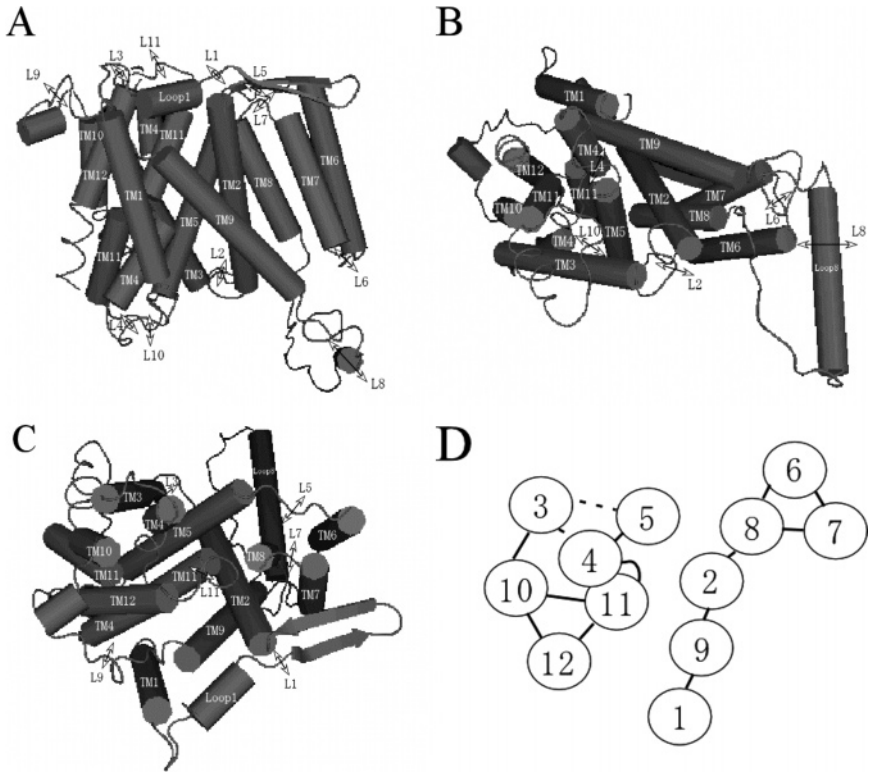

FIGURE 9: Locations of each TM domains in the HPNhaA structure estimated from *E. coli* crystal structure. The HPNhaA structure is viewed from the middle of the membrane (A), from the cytoplasmic side (B), or from the periplasmic side (C) of the protein. The proximity of each TM is shown schematically in (D).

with their complementary fragments and are then stabilized by the interaction.

The reconstituted NhaA showed high activity in the Na^+/H^+ antiport between pH 6.5 and pH 8.5 for most of the fragment pairs, but the reconstituted Li^+/H^+ antiporter activity was lower than the Na^+/H^+ activity especially at alkaline pH (Figure 7). These results suggest that the reconstitution is partly successful, but that the reconstituted structure may not be exactly the same as the wild type. We have previously reported differences in activity between Na^+/H^+ and Li^+/H^+ antiports in a chimeric NhaA constructed from ECNhaA and HPNhaA. In the chimera, Li^+/H^+ activity was lower than Na^+/H^+ activity (*30*), as observed here. Interaction of NhaA monomers within an oligomer (detected by FRET) indicated that interactions between monomers were weakened by Li^+ binding but not by Na^+ binding (*29*). These observations suggested that Li^+ binding and/or a conformational change propagated by Li^+ binding may differ from changes induced by Na^+ binding. The present results are consistent with differential ion binding of Na^+ and Li^+ by NhaA. Furthermore, the pH-dependent Li^+/H^+ and Na^+/H^+ antiporter activity profiles differ between the intact and the reconstituted NhaA. At alkaline pH values, Li^+/H^+ antiporter activity is much lower than the basal level (Figure 7) for the L2 pair. Li^+ caused increased accumulation of H^+ inside the vesicles (Figure 7). This result suggested that Li^+ binding did not cause H^+ efflux by the antiport mechanism, but rather blocked H^+ efflux, while H^+ influx continued due to lactate respiration. The total extent of fluorescence quenching is lower for the reconstituted NhaA than for the wild type, suggesting that the reconstituted NhaA is leaky to H^+. These interesting features of reconstituted NhaA will provide a useful tool for the study of Na^+/H^+ exchange mechanisms.

ACKNOWLEDGMENT

We thank Dr. Atsushi Miyawaki (Riken Institute for Brain Research) for providing the Venus GFP variant.

REFERENCES

1. Padan, E., and Schuldiner, S. (1992) *Alkali Cation Transport System in Procaryotes* (Bakker, E., Ed.) pp 3−24, CRC Press, Inc., Boca Raton, FL.
2. Padan, E., and Schuldiner, S. (1994) Molecular physiology of Na^+/H^+ antiporters, key transporters in circulation of Na^+ and H^+ in cells, *Biochim. Biophys. Acta 1185*, 129−151.
3. Schuldiner, S., and Padan, E. (1992) *Alkali Cation Transport Systems in Procaryotes* (Bakker, E., Ed.) pp 25−51, CRC Press, Inc., Boca Raton, FL.
4. Padan, E. (1998) *Microbiology and Biochemistry of Hyper Saline Environments* (Oren, A., Ed.) pp 163−175, CRC Press, Inc., Boca Raton, FL.
5. Karpel, R., Olami, Y., Taglicht, D., Schuldiner, S., and Padan, E. (1988) Sequencing of the gene *ant* which affects the Na^+/H^+ antiporter activity in *Escherichia coli*, *J. Biol. Chem. 263*, 10408−10414.
6. Pinner, E., Padan, E., and Schuldiner, S. (1992) Cloning, sequencing, and expression of the *nhaB* gene, encoding a Na^+/H^+ antiporter in *Escherichia coli*, *J. Biol. Chem. 267*, 11064−11068.
7. Ivey, D. M., Guffanti, A. A., Zemsky, J., Pinner, E., Karpel, R., Padan, E., Schuldiner, S., and Krulwich, T. A. (1993) Cloning and characterization of a putative Ca^{2+}/H^+ antiporter gene from *Escherichia coli* upon functional complementation of Na^+/H^+ antiporter- deficient strains by the overexpressed gene, *J. Biol. Chem. 268*, 11296−11303.
8. Taglicht, D., Padan, E., and Schuldiner, S. (1991) Overproduction and purification of a functional Na^+/H^+ antiporter coded by *nhaA* (*ant*) from *Escherichia coli*, *J. Biol. Chem. 266*, 11289−11294.

9. Pinner, E., Padan, E., and Schuldiner, S. (1994) Kinetic properties of NhaB, a Na^+/H^+ antiporter from *Escherichia coli*, *J. Biol. Chem. 269*, 26274−26279.
10. Rothman, A., Padan, E., and Schuldiner, S. (1996) Topological analysis of NhaA, a Na^+/H^+ antiporter from *Escherichia coli*, *J. Biol. Chem. 271*, 32288−32292.
11. Inoue, H., Noumi, T., Sakurai, T., Tsuchiya, T., and Kanazawa, H. (1995) Essential aspartic acid residues, Asp-133, Asp-163 and Asp-164, in the transmembrane helices of a Na^+/H^+ antiporter (NhaA) from *Escherichia coli*, *FEBS Lett. 363*, 264−268.
12. Tsuboi, Y., Inoue, H., Nakamura, N., and Kanazawa, H. (2003) Identification of membrane domains of the Na^+/H^+ antiporter (NhaA) protein from *Helicobacter pylori* required for ion transport and pH sensing, *J. Biol. Chem. 278*, 21467−21473.
13. Inoue, H., Sakurai, T., Ujike, S., Tsuchiya, T., Murakami, H., and Kanazawa, H. (1999) Expression of functional Na^+/H^+ antiporters of *Helicobacter pylori* in antiporter-deficient *Escherichia coli* mutants, *FEBS Lett. 443*,11−16.
14. Kuwabara, N., Inoue, H., Tsuboi, Y., Nakamura, N., and Kanazawa, H. (2004) The fourth transmembrane domain of the *Helicobacter pylori* Na^+/H^+ antiporter NhaA faces a water-filled channel required for ion transport, *J. Biol. Chem. 279*, 40567−40575.
15. Kuwabara, N., Inoue, H., Tsuboi, Y., Mitsui, K., Matsushita, M., and Kanazawa, H. (2006) Structure-function relationship of the fifth transmembrane domain in the Na^+/H^+ antiporter of *Helicobacter pylori*: Topology and function of the residues, including two consecutive essential aspartate residues, *Biochemistry 45*, 14834−14842.
16. Hunte, C., Screpanti, E., Venturi, M., Rimon, A., Padan, E., and Michel, H. (2005) Structure of a Na^+/H^+ antiporter and insights into mechanism of action and regulation by Ph, *Nature 435*, 1197−1201.
17. Galili, L., Herz, K., Dym, O., and Padan, E. (2004) Unraveling functional and structural interactions between transmembrane domains IV and XI of NhaA Na^+/H^+ antiporter of Escherichia coli, *J. Biol. Chem. 279*, 23104−23113.
18. Popot, J. L., and Engelman, D. M. (1990) Membrane protein folding and oligomerization: the two-stage model, *Biochemistry 29*, 4031−4037.
19. Engelman, D. M., Chen, Y., Chin, C. N., Curran, A. R., Dixon, A. M., Dupuy, A. D., Lee, A. S., Lehnert, U., Matthews, E. E., Reshetnyak, Y. K., Senes, A., and Popot, J. L. (2003) Membrane protein folding: beyond the two stage model, *FEBS Lett. 555*, 122−125.
20. Groves, J. D., and Tanner, M. J. A., (1995) Co-expressed complementary fragments of the human red cell anion exchanger (band 3, AE1) generate stilbene disulfonate-sensitive anion transport, *J. Biol. Chem. 270*, 9097−9105.
21. Wang, J. D., Groves, J. D., Mawby, W. J., and Tanner, M. J. A. (1997) Complementation studies with co-expressed fragments of the human red cell anion transporter (band 3; AE1). The role of some exofacial loops in anion transport, *J. Biol. Chem. 272*, 10631−10638.
22. Groves, J. D., Wang, L., and Tanner, M. J. A. (1998) Functional reassembly of the anion transport domain of human red cell band 3 (AE1) from multiple and non-complementary fragments, *FEBS Lett. 433*, 223−227.
23. Martin, N. P., Leavitt, L. M., Sommers, C. M., and Dumont, M. E. (1999) Assembly of G protein-coupled receptors from fragments: identification of functional receptors with discontinuities in each of the loops connecting transmembrane segments, *Biochemistry 38*, 682−695.
24. Bibi, E., and Kaback, H. R. (1990) In vivo expression of the lacY gene in two segments leads to functional lac permease, *Proc. Natl. Acad. Sci. U.S.A. 87*, 4325−4329.
25. Yamaguchi, A., Someya, Y., and Sawai, T. (1993) The in vivo assembly and function of the N- and C-terminal halves of the Tn10-encoded TetA protein in *Escherichia coli*, *FEBS Lett. 324*, 131−135.
26. Thelen, P., Tsuchiya, T., and Goldberg, E. B. (1991) Characterization and mapping of a major Na^+/H^+ antiporter gene of *Escherichia coli*, *J. Bacteriol. 173*, 6553−6557.
27. Messing, J., and Vieira, J. (1982) A new pair of M13 vectors for selecting either DNA strand of double-digest restriction fragments, *Gene (Amsterdam) 19*, 269−276.
28. Kanazawa, H., Miki, T., Tamura, F., Yura, T., and Futai, M. (1979) Specialized transducing phage lambda carrying the genes for coupling factor of oxidative phosphorylation of *Escherichia coli*: increased synthesis of coupling factor on induction of prophage lambda asn, *Proc. Natl. Acad. Sci. U.S.A. 76*, 1126−1130.
29. Karasawa, A., Tsuboi, Y., Inoue, H., Kinoshita, R., Nakamura, N., and Kanazawa, H. (2005) Detection of oligomerization and conformational changes in the Na^+/H^+ antiporter from *Helicobacter pylori* by fluorescence resonance energy transfer, *J. Biol. Chem. 280*, 41900−41911.
30. Inoue, H., Tsuboi, Y., and Kanazawa, H. (2001) Chimeric Na-(+)/H(+) antiporters constructed from NhaA of *Helicobacter pylori* and *Escherichia coli*: implications for domains of NhaA for pH sensing, *J. Biochem. 129*, 569−576.
31. Nozaki, K., Inaba, K., Kuroda, T., Tsuda, M., and Tsuchiya, T. (1996) Cloning and sequencing of the gene for Na^+/H^+ antiporter of *Vibrio parahaemolyticus*, *Biochem. Biophys. Res. Commun. 222*, 774−779.
32. Maniatis, T., Fritsch, F., and Sambrook, J. (1982) *Molecular Cloning: A Laboratory Manual*, Cold Spring Harbor Laboratory, Cold Spring Harbor, NY.
33. Ito, K., and Akiyama, Y. (2005) Cellular functions, mechanism of action, and regulation of FtsH protease, *Annu. Rev. Microbiol. 59*, 211−231.
34. Okuno, T., Yamada-Inagawa, T., Karata, K., Yamanaka, K., and Ogura, T. (2004) Spectrometric analysis of degradation of a physiological substrate σ^{32} by *Escherichia coli* AAA protease FtsH, *J. Struct. Biol. 146*. 148−154.
35. Sakaguchi, M. (2002) Autonomous and heteronomous positioning of transmembrane segments in multispanning membrane protein, *Biochem. Biophys. Res. Commun. 296*, 1−4.
36. Schmidt-Rose, T., and Jentsch, T. J. (1997) Reconstitution of functional voltage-gated chloride channels from complementary fragments of CLC-1, *J. Biol. Chem. 272*, 20515−20521.
37. Chan, K. W., Csanady, L., Seto-Young, D., Nairn, A. C., and Gadsby, D. C. (2000) Severed molecules functionally define the boundaries of the cystic fibrosis transmembrane conductance regulator's NH(2)-terminal nucleotide binding domain, *J. Gen. Physiol. 116*, 163−180.
38. Liao, M. J., Huang, K. S., and Khorana, H. G. (1984) Regeneration of native bacteriorhodopsin structure from fragments, *J. Biol. Chem. 259*, 4200−4204.
39. Marti, T. (1998) Refolding of bacteriorhodopsin from expressed polypeptide fragments, *J. Biol. Chem. 273*, 9312−9322.
40. Ridge, K. D., Lee, S. J., and Yao, L. L. (1995) In vivo assembly of rhodopsin from expressed polypeptide fragments, *Proc. Natl. Acad. Sci. U.S.A. 92*, 3204−3208.
41. Ridge, K. D., Lee, S. S., and Abdulaev, N. G. (1996) Examining rhodopsin folding and assembly through expression of polypeptide fragments, *J. Biol. Chem. 271*, 7860−7867.
42. Zen, K. H., McKenna, E., Bibi, E., Hardy, D., and Kaback, H. R. (1994) Expression of lactose permease in contiguous fragments as a probe for membrane-spanning domains, *Biochemisty. 33*, 8198−8206.
43. Kohl, B., Wagner, C. A., Huelseweh, B., Busch, A. E., and Werner, A. (1998) The Na^+-phosphate cotransport system (NaPi-II) with a cleaved protein backbone: implications on function and membrane insertion, *J. Physiol. 508*, 341−350.
44. Wilkinson, B. M., Esnault, Y., Craven, R. A., Skiba, F., Fieschi, J., Kepes, F. and Stirling, C. J. (1997) Molecular architecture of the ER translocase probed by chemical crosslinking of Sss1p to complementary fragments of Sec61p, *EMBO J. 16*, 4549−4559.
45. Ridge, K. D., Ngo, T., Lee, S. S. J., and Abdulaev, N. G. (1999) Folding and assembly in rhodopsin. Effect of mutations in the sixth transmembrane helix on the conformation of the third cytoplasmic loop, *J. Biol. Chem. 274*, 21437−21442.

BI701627E